Check for updates

A rigid plant oil-based thermoset with a furfural-derived cyclobutane cross-linker†

Jonathan Tellers, Nicolas Sbirrazzuoli [ID] and Nathanael Guigo [ID] *

Bio-based hardeners that are not amine or anhydride based are of particular interest to avoid associated health concerns. In the present study, a recently developed furfural-based cross-linker bearing a semi-rigid cyclobutane moiety is investigated for its capacity to cross-link epoxidized linseed oil, resulting in a wholly bio-based thermoset. The kinetics of the curing process are elucidated, as well as the mechanical properties of the resulting material. The cured thermoset displayed particularly high tensile strength and a high glass transition for a flexible triglyceride-based network, exceeding that of many previously published di-acid thermosets.

Introduction

Spurred on by a paradigm shift in the mindset of consumers, media and policy-makers, researchers have been encouraged to develop sustainable materials that can act as an alternative to the current fossil-based solutions, and thus to design the circular economy process from the ground up.[1,2]

As such, a strong emphasis has been placed on biomass-derived chemicals and entities. The US government has identified key chemicals of the biorefinery process and is encouraging research into these particular chemicals.[3] The idea is to use chemicals that are side-products of biofuel production to allow for the establishment of a biobased industry in addition to obtaining materials with unique properties such as their degradability to harmless natural components.[4]

Furans, such as 5-(hydroxymethyl)furfural (HMF)[5] and furfural,[6,7] are examples of the key chemicals that have been identified in this manner, having been obtained from the dehydration of sugars and various other biological sources.[3,6] They have recently been employed in the development of sustainable and economically viable chemicals and materials.[8,9] Furfural is of particular interest, as it is commercially available at a larger scale and is the sole precursor for chemicals comprising a furyl, furfuryl, furoyl or furfuylidene group in the chemical industry.[10,11] It has thus been used to make a plethora of precursor molecules for novel polymers and other furyl containing chemicals.[12]

Recently, furfural-derived *trans*-3-(2-furyl)acrylic acid (FAA)[13,14] has been used to develop a novel type carboxylic di-acid, namely **CBDA-2** (*cis*-cyclobutane-1,2-dicarboxylic acid),[15] which can be used as a green, semi-rigid cross-linker. While the researchers mentioned the possibility of using **CBDA-2** in conjunction with epoxy resins, they only briefly explored a coating using epoxidized sucrose soyate and, furthermore, relied on methanol as a solvent instead of following a green, solvent-free procedure, as demonstrated in the present paper (*vide infra*). While sufficient to prove the concept, epoxidized linseed oil (ELO) is by far the predominant choice for bio-based epoxidized matrices, because it can be obtained by green methods, and is both cheap, and industrially available.[16–18] To benefit from such a promising natural epoxy matrix, innovation in the field of bio-based hardeners is required, and has gained significant traction in recent years.[19–22]

In the current study, we investigate the ability of **CBDA-2** to cross-link ELO in a hot curing procedure in the absence of any solvent. We analyze the kinetics of the process and the properties of the resulting thermosets, which are compared to the previously described thermosets that have been obtained through sustainable cross-linkers.

Materials and methods

Materials

Epoxidized linseed oil (ELO) was kindly provided by Valtris Chemicals (molecular weight of 980 g mol^{-1}. The average of 5.5 epoxy groups per molecule was determined by the supplier by means of non-aqueous potentiometric titration (ASTM D 1652). Furylacrylic acid (99%) and hexane (puriss, 2.5 L) were purchased from Sigma-Aldrich (now MERCK) and used as received. Two LED UV 50 W black lights were purchased from Amazon.

Institut de Chimie de Nice, Université Côte d'Azur, CNRS, UMR 7272, 06108 Nice, France. E-mail: Nathanael.GUIGO@univ-cotedazur.fr

†Electronic supplementary information (ESI) available: NMR spectra and supplementary rheological, FTIR, and DMTA data. See DOI: 10.1039/d0gc04323k

Synthesis of *cis*-cyclobutane-1,2-dicarbocylic acid (CBDA-2)

The procedure was adapted from the literature.[15] The photosynthesis step was carried out in an 500 mL Erlenmeyer flask: 25 g of crystalline 3-(2-furyl) acrylic acid was ground into a fine power using a mortar and pestle. The acid was suspended in 250 mL of hexane in the flask and stirred vigorously. The suspension was irradiated overnight using two 50-watt black lights (395–400 nm). Occasionally, the powder that stuck to the inside wall of the flask was loosened using a spatula. The slurry was then filtered, and an off-white solid was obtained (24.2 g, 97%). The filtered hexane was kept in order to be reused for future reactions. In the case where NMR revealed an uncompleted reaction (observed on one occasion), the powder was suspended again and irradiated for another night, which resulted in complete conversion of the starting material. ^{1}H-NMR (DMSO-d_6, 400 MHz) δ 12.56 (s, 2H), 7.40 (m, 2H), 6.25 (m, 2H), 6.11 (d, J = 3.2 Hz 2H), 4.04 (m, 2H), 3.67 (m, 2H); see also Fig. S1† for the NMR spectrum.

The precise number of epoxy groups in the ELO and its molecular weight were determined by NMR (Fig. S1†). The integration of the single glycerol CH was set as 1, which allows one to determine the number of epoxy groups per molecule according to eqn (1):

$$N_{\text{epoxy}} = \left(\frac{\int \text{oxirane}}{2}\right) = \frac{6.01 + 3.72 + 1.36}{2} = 5.545 \quad (1)$$

and the average molecular weight of ELO according to eqn (2):

$$M_{\text{ELO}} = M_{\text{glycidyl ester}} + \left(\frac{M_{-\text{CC}-} \times \int -\text{CC}-}{N_{\text{proton}}}\right)$$
$$+ \left(\frac{M_{\text{oxirane}} \times \int \text{oxirane}}{N_{\text{proton}}}\right) + \left(\frac{M_{-\text{CH}_3} \times \int -\text{CH}_3}{N_{\text{proton}}}\right)$$
$$+ \left(\frac{M_{-\text{CH}_2-} \times \int -\text{CH}_2-}{N_{\text{proton}}}\right)$$
$$M_{\text{ELO}} = 173.1 \, \text{g mol}^{-1} + \left(\frac{26.038 \, \text{g mol}^{-1} \times 0.215}{2}\right) \quad (2)$$
$$+ \left(\frac{42.037 \, \text{g mol}^{-1} \times 11.09}{2}\right)$$
$$+ \left(\frac{15.035 \, \text{g mol}^{-1} \times 9}{3}\right)$$
$$+ \left(\frac{14.072 \, \text{g mol}^{-1} \times 69.75}{2}\right) = 944.86 \, \text{g mol}^{-1}$$

The amount of required **CBDA-2** for 25 g ELO is calculated as follows (eqn (3)):

$$m_{\text{CBDA}} = \left(\frac{m_{\text{ELO}}}{M_{\text{ELO}}}\right) \times N_{\text{epoxy}} \times R_{\text{ELO}} \times \left(\frac{M_{\text{CBDA}}}{N_{\text{COOH}}}\right)$$
$$m_{\text{CBDA}} = \left(\frac{25 \, \text{g}}{944.86 \, \text{g mol}^{-1}}\right) \times 5.545 \times 0.8 \times \left(\frac{276.24}{2}\right) \quad (3)$$
$$= 16.2 \, \text{g CBDA}$$

ELO and **CBDA-2** were mixed using a spatula, forming a brown sludge with a viscosity similar to a cake dough. This mixture was transferred into the appropriate mold and degassed by floating in a sonicating bath for 1 h. The mixture was then cured in an oven in a two-step curing process. First, 1 h at 110 °C, then 2 h at 130 °C. Full consumption of oxirane groups was confirmed *via* IR and ^{13}C solid-state NMR.

Nuclear magnetic resonance (NMR)

NMR spectra were recorded on a Bruker AVANCE III (400 MHz). ^{1}H-NMR chemical shifts are given in reference to the residual solvent peak of CDCL$_3$ at 7.26 ppm or DMSO_d_6 at 2.50 ppm. The solid-state ^{13}C spectra were obtained on a Bruker Avance-400 MHz NMR spectrometer (magnetic field 9.4 T) using a double channel Bruker probe. About 100 mg of sample was placed in zirconium dioxide rotor of 4 mm outer diameter and spun at a magic angle spinning rate of 10 kHz and 4 kHz for solid and liquid samples, respectively. For the solid samples, the CPMAS technique (Schaefer and Stejskal, 1976) was applied with a ramped 1H-pulse starting at 100% power and decreasing until 50% during the contact time (2 ms) in order to circumvent Hartmann–Hahn mismatches. To obtain a good signal-to-noise ratio in ^{13}C CPMAS experiment 10k scans were accumulated using a delay of 2.5 s. For ^{13}C single pulse experiment (SPE) the acquisition parameters were 3.4 μs 45° pulse, 2 s recycle delay and 1024 scans. The ^{13}C chemical shifts were referenced to tetramethyl silane and calibrated with glycine carbonyl signal, set at 176.03 ppm.

Rheology

Curing studies were performed on a Thermo Scientific HAAKE MARS rheometer. Isothermal curing measurements were obtained in plate–plate geometry (25 mm diameter, 1 mm gap, 0.5% strain) at varying temperatures (90, 95, 100, 110, 120, and 130 °C). Variations of complex viscosity and storage and loss modulus with temperature were analyzed.

Dynamic mechanical thermal analysis (DMTA)

The dynamic mechanical properties were studied using a Mettler-Toledo DMA-1 in tensile mode. Samples were tested in temperature sweeps from −100 °C to 180 °C with a heating rate of 2 °C min^{-1}. Experiments were done in a single frequency oscillation mode with a frequency of 1 Hz, a force amplitude of 0.1 N and a displacement amplitude of 0.1% in auto-tension offset control. Multi-frequency DMTA experiments were conducted at 1 °C min^{-1} with a displacement amplitude of 0.1% between 0.1 Hz and 10 Hz.

Shore D hardness test

The hardness of the rubbers was determined using Shore D type durometers, which are used for hard rubbers.[23] The hardness was determined according to ASTM D2240.

Tensile tests

Tensile tests were performed with a Shimadzu EZ-LX tensile tester equipped with a 1 kN load cell. The tests were performed on dog bones (l = 48 mm, w = 5.1–5.3 mm, t = 1.9–3.5 mm) cut from cured 19.6 × 19.6 cm square slabs of the respective material. The exact sample dimensions were determined for

each sample before testing. A grip-to-grip separation of 35.92 mm was used. The samples were prestressed to 0.1 N and then loaded with a constant crosshead speed of 20 mm min^{-1}.

Differential scanning calorimetry (DSC)

DSC measurements were performed with a Mettler-Toledo DSC823^{e} heat-flux instrument. STAR software was used for data analysis. Temperature, enthalpy, and tau lag calibrations were performed with indium and zinc standards. Freshly mixed **CBDA-2**/ELO samples (10–20 mg) were placed in a 40 mL aluminum crucible and closed with a punctured pan lid. The experiments were done under air flow (80 mL min^{-1}). Curing of the mixtures was studied under isothermal conditions at 100, 105, 110, 120, 130 °C, followed by a second scan at 10 °C min^{-1} in order to determine the glass transition (T_g) from the inflection point of the specific heat capacity (C_p) increment. The DSC experiments were conducted according to the ICTAC Kinetics Committee recommendations for collecting thermal analysis data for kinetic computations and were performed using an advanced isoconversional method applied to the dataset obtained from isothermal DSC measurements.[24,25]

Theoretical considerations

Isoconversional methods have been widely used to study complex cure mechanisms.[26–28] Polymerizations are frequently monitored by DSC. In this case, the extent of conversion is computed according to eqn (4), as follows:

$$\alpha_t = \frac{\int_{t_i}^{t} (dQ/dt)dt}{\int_{t_i}^{t_f} (dQ/dt)dt} = \frac{Q_t}{Q_{tot}} \tag{4}$$

where α_t, represents the extent of conversion at time t, t_i represents the time of the first integration bound of the DSC signal and t_f the time of the last integration bound selected when the reaction is finished. dQ/dt is the heat flow measured by DSC at time t, Q_{tot} is the total heat released (or absorbed) by the reaction and Q_t is the current heat change.

The general form of the basic rate equation to kinetic analysis of the condensed phase processes is usually written as given in literature:[24]

$$\frac{d\alpha}{dt} = k(T)f(\alpha) = A \exp\left(-\frac{E}{RT}\right) \tag{5}$$

The advanced non-linear isoconversional method (NLN) or Vyazovkin's method used in this study is presented in eqn (6) and (7) and has been derived from eqn (5):[29–32]

$$\Phi(E_\alpha) = \sum_{i=1}^{n} \sum_{j\neq i}^{n} \frac{J[E_\alpha, T_i(t_\alpha)]}{J[E_\alpha, T_j(t_\alpha)]} \tag{6}$$

$$J[E_\alpha, T(t_\alpha)] \equiv \int_{t_{\alpha-\Delta\alpha}}^{t_\alpha} \exp\left[\frac{-E_\alpha}{RT(t)}\right]dt \tag{7}$$

where E_α is the effective activation energy. The E_α value is determined as the value that minimizes the function $\Phi(E_\alpha)$.

This method was implemented in an internally generated software.[30,32,33] The computations yield the values of effective activation energy E_α as a function of extent of conversion α evaluated without assumption on the reaction mechanism. It has previously been shown that E_α-dependencies allow for meaningful mechanistic analyses and the elucidation of multi-step processes.[26–28]

Results and discussion

To obtain a potential green alternative to current hardener technologies, it must be possible to obtain all components by green methods. **CBDA-2** can be obtained by starting from the furfural-derived *trans*-3-(2-furyl)acrylic acid through a formation of a four-membered ring facilitated by irradiation using a simple commercially available black light (Fig. 1). For the synthesis described here, a scaled-up version of the procedure described in literature was used,[15] employing hexane to float the furylacrylic acid, so that the reaction can proceed in the solid under blacklight irradiation (395–400 nm) with commercially available lights.

The hexane that was used during the reaction can be reused in subsequent synthesis, thereby avoiding waste due to discarded solvent. In the future, other liquids could be explored to suspend the acid, including those which are obtained from natural resources. **CBDA-2** is obtained as a fine powder after filtering, and can be readily mixed with an epoxy matrix without further need for grinding.

As an epoxy, we chose epoxidized linseed oil (ELO), a green epoxy matrix with high epoxy units content relative to other natural oils.[16] From previous investigations,[20,34] we know that the highest enthalpy release is observed when a ratio of 0.8 epoxy groups to COOH groups is used. The molecular weight and epoxy group content of ELO was calculated by NMR (spectra in Fig. S2†), and the appropriate amount of **CBDA-2** was calculated accordingly (details in the Experimental section). After thorough mixing of ELO and **CBDA-2** for a couple of minutes, a brown slush forms (Fig. S3†), which can be poured into a negative mold with the desired shape. The curing behavior of the ELO/**CBDA-2** mixture was initially investigated using DSC measurements. A dynamic DSC scan (Fig. S4†) revealed that the reaction starts at around 90 °C, with a peak of DSC heat flow observed at 136 °C, which is proportional to the reaction rate. Furthermore, we observe a T_g of 19 °C for the cured material.

Fig. 1 Scheme of **CBDA-2** synthesis from furfural derived *trans*-3-(2-furyl)acrylic acid.

Isothermal curing was subsequently carried out using a rheometer and DSC at multiple temperatures below the observed peak to study curing kinetics and to identify an appropriate curing program to obtain test specimens for mechanical testing. Isothermal curing on a parallel plate rheometer was carried at different temperatures and monitored until the storage modulus (G') started to plateau. The individual curing experiments are displayed in Fig. S5.† We can see that, even at 90 °C, the curing reaction is initiated. In a previous study,[15] **CBDA-2** is given a melting point of 170–171 °C but according to our DSC analyses, we observed a melting point of 180 °C. Given that the reaction starts much earlier, it is clear that **CBDA-2** either dissolves in ELO or, more likely, that they form an eutectic mixture exhibiting a lower melting point, allowing the reaction to proceed at temperatures below the melting point of the acid. This has already been observed in other studies where ELO was cured with the powder of a solid acid.[34] The reaction proceeds very quickly at temperatures above 110 °C, reaching a G' plateau after about 2 h. Using the gel point obtained at different temperatures, the activation energy (E_A) at the point of gelation can be determined. Because the conversion α is generally identical at the gel point (t_{gel}), one can calculate the E_A using the Arrhenius relation:[35–38]

$$\ln t_{\alpha,gel} = C + \frac{E_A}{RT_i} \quad (8)$$

with C as a constant and R as the universal gas constant. Fitting a plot of $\ln(t_{\alpha,gel})$ against $1/T$ allows one to determine the E_A from the slope of that fit. The plot of $\ln(t_{\alpha,gel})$ *vs.* $1000/T_i$ for each of the measured formulations is given in Fig. 2. Thereby, an E_A of 81 kJ mol^{-1} was determined, which is in line with other curing reactions of epoxy matrices.[19,20]

Subsequent isothermal curing tests were carried out on the calorimeter, followed by determination of the T_g reached during the protocol. To achieve this, each sample was sub-
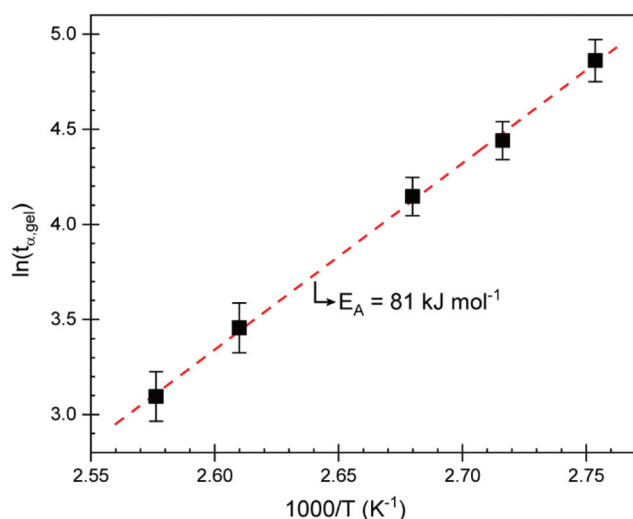

Fig. 2 Plot of the logarithm of the time it took to reach the gel point ($t_{\alpha,gel}$) *vs.* the inverse isothermal curing temperature.

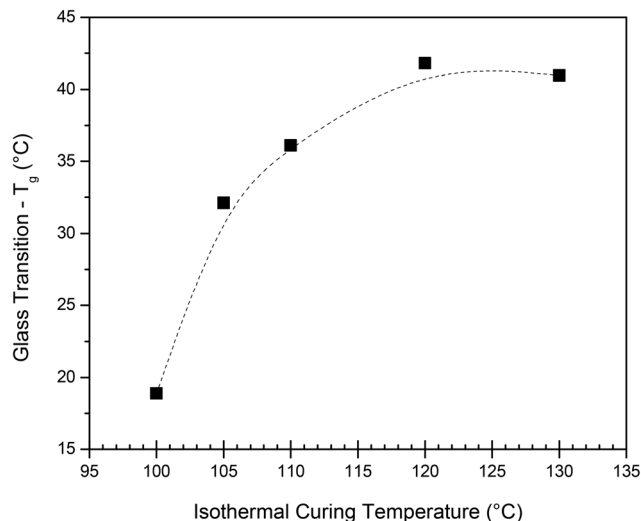**Fig. 3** Obtained T_g of samples cured for 2 h at different isothermal curing temperatures. The T_g was determined immediately after the isothermal curing of the samples by cooling and heating the samples at 10 K min^{-1}.

jected to the respective isothermal curing temperature for 2 h, cooled down, followed by immediate determination of the T_g (details in the Experimental section). In Fig. 3, the obtained T_g is plotted as a function of the applied isothermal curing temperature. Two hours at $T > 120$ °C proved sufficient to obtain full curing, as the T_g of the sample cured at 120 °C and 130 °C gave a similar value. For the lower temperatures, a lower T_g was obtained in the 2 h timeframe, suggesting that it is insufficient to fully cure the system. The T_g obtained during the dynamic curing experiment is about 20 °C lower than that obtained during the isothermal curing experiment performed at 130 °C. It has previously been reported[39] that the cyclobutane ring can undergo thermocleavage at high temperatures, which would lead to an overall reduced cross-link density and a T_g of the final polymer. This could be a potential reason for the observed lower T_g and should be considered during sample preparation.

The data obtained from isothermal curing were also used to determine the effective activation energy as a function of the extent of conversion α using the advanced isoconversional method (eqn (2) and (3)). The resulting E_α is plotted in Fig. 4.

According to Flory,[40] the conversion at which the gel point is reached is only dependent on the functionality of the epoxy resin and the hardener, according to the following relation:

$$\alpha_{gel} = \left(\frac{1}{(F_A - 1)(F_E - 1)}\right)^{\frac{1}{2}} = \left(\frac{1}{(5.5 - 1)(2 - 1)}\right)^{\frac{1}{2}} = 0.5$$

where F_A and F_E are the respective functionalities of the epoxy and carboxylic acid. With 5.5 epoxy functionalities on every ELO molecule, we thus estimate an α_{gel} of 0.47 ± 0.04, which gives an E_α at $t_{\alpha,gel}$ of 87 ± 5 kJ mol^{-1}, as indicated in Fig. 4. The previously conducted rheology tests (see above) investigated the activation energy at the gel point, and the obtained
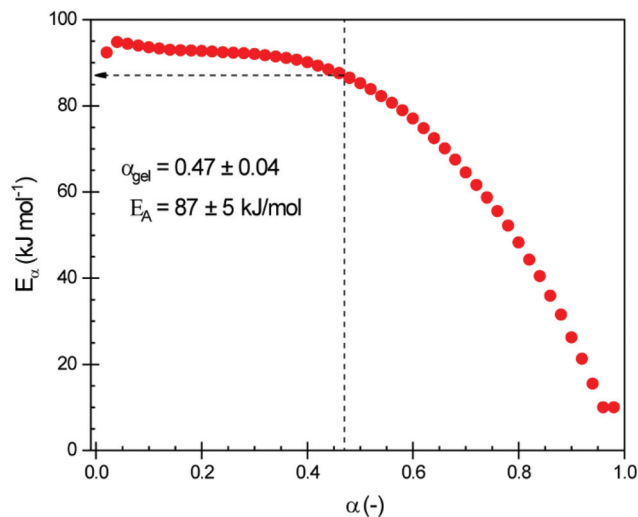
Fig. 4 Dependence of the effective activation energy (E_α) with extent of conversion (α).

value of 81 ± 5 kJ mol^{-1} is very close to the one determined here by DSC experiments. The difference can be explained by the approximation of a constant value of E_A to obtain eqn (8) after integration of eqn (5).

At low conversions, the curing is controlled by the chemical reactions, and has a high activation energy (around 95 kJ mol^{-1}). Values of around 125–140 kJ mol^{-1} were reported by Menager et al. for the ring opening of epoxidized linseed oil with three aliphatic biobased dicarboxylic acids (i.e., succinic, suberic and sebacic acids).[34] As the reaction processes and the material vitrifies, diffusion becomes the factor that dominates the reaction rate, which lowers the activation energy as diffusion processes have a lower activation energy.[37,41] It has been shown that diffusion control can occur for the extent of conversion close to 0.3–0.4 [37] and that the onset of the diffusion regime can be associated with gelation rather than vitrification.[42]

Analysis of the data displayed in Fig. 4 shows that for this system diffusion control starts at around $\alpha = 0.4$–0.5, i.e., well below vitrification and around gelation. This is explained by the constrained chemical structure of **CBDA-2**.

To obtain samples without entrapped air that are fully cured, we devised the following curing procedure: specimens were cured in a two step-process, first at 110 °C for 1 h, followed by a post curing step at 130 °C for an additional 2 h. FTIR of samples prepared in this manner revealed full consumption of the epoxy groups, judging from the disappearance of the oxirane group band at 821 cm^{-1} (Fig. S6†). In addition, solid-state ^{13}C NMR investigations were conducted to highlight structural modifications during the cross-linking. The spectra of both, ELO and the cured **CBDA-2**/ELO resins are shown in Fig. S7.† Interestingly, the resonances associated to the oxirane groups in ELO ($55 < \delta < 59$ ppm) have disappeared in the spectrum of the cross-linked resin confirming the full consumption of the epoxy group. Instead new resonances appears

in the 65–85 ppm region confirming the formation of β-hydroxyester throughout the epoxy ring opening during the cross-linking between ELO and **CBDA-2**. The resonances observed in the cured sample respectively at $\delta = 107.4$; 110.6; 142.1; 153.2 ppm correspond to the sp^2 carbons from the furanic ring in CBDA. In order to obtain suitable sample specimens, a prepared mixture of ELO and **CBDA-2** was poured in a rectangular mold with a dimension of 10×10 cm and degassed using sonication, followed by curing using the aforementioned curing sequence, yielding solid thermoset slabs. These slabs could be used to cut dog bones and rectangular strips using a CNC router to obtain samples suitable for TGA, tensile testing and DMTA measurements. First, the TGA scan of cured **CBDA-2**/ELO thermosets is shown in Fig. S8† together with the one of the diacid **CBDA-2**. It highlights that the diacid starts to decompose above 200 °C. The temperature corresponding to 5% of total decomposition – i.e. $T_{5\%} = 210$ °C for neat **CBDA-2** while the $T_{5\%}$ increases to 270 °C for the cured resin. It confirms on one hand that the chosen curing conditions (110 °C; 130 °C) are well below 200 °C and thus it should prevent decomposition of CBDA during cross-linking. On the other hand the $T_{5\%}$ of **CBDA-2**/ELO is comparable to those of ELO cured with 2,2′-dithiodibenzoic acid[43] and lower compared to systems cross-linked with adipic acid or glutaric anhydride ($T_{5\%}$ ~340 °C) as these linear organic diacid are less prone to decomposition.[22]

The resulting DMTA data is displayed in Fig. 5. We observe a T_g at 53 °C (peak of tan δ), explaining the rigid nature of the material at room temperature. This value is significantly above that which can be achieved with green aliphatic multifunctional carboxylic acids[19] or common anhydrides such as maleic anhydride (MA).[44] **CBDA-2** is outperformed by more rigid fossil-based anhydrides such as methyl tetrahydrophthalic anhydride (MTHPA),[45] and **CBDA-2** can thus be employed as a semi-rigid hardener. A plateau modulus of 4.6 MPA at
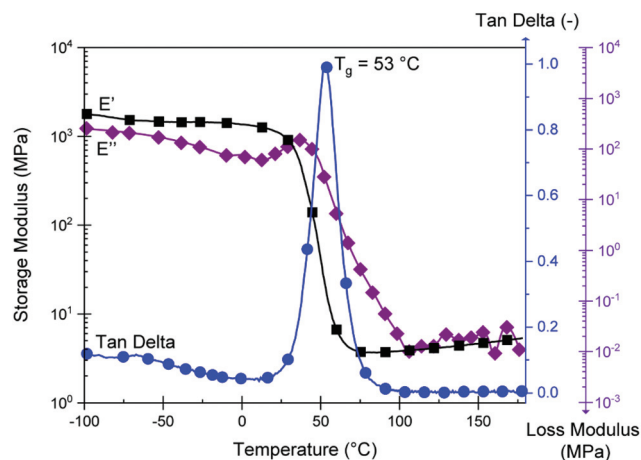

Fig. 5 DMTA data (−100 °C to 180 °C, 1 Hz, 0.1% strain) of cured **CBDA-2**/ELO thermosets using a fixed COOH/oxirane group-ratio of 0.8 (the symbols are intended to help differentiate the curves and do not represent the sole data points).

150 °C is observed. Using the classical theory of rubber elasticity,[46,47] one can determine the molecular weight between cross-links (M_c) according to the following relationship:

$$M_c = \frac{3\rho RT}{E'_T} \qquad (9)$$

With ρ as the Poisson's ratio (for linseed oil estimated at of 0.34 [48–51]), R as the general gas constant, and E'_T as the storage modulus for a temperature $T = T_g + 30$ within the rubber plateau modulus. We thus calculate a value of $M_c = 775$ g mol^{-1}, which is similar to findings from other publications where epoxidized linseed oils are used as a matrix.[52,53] As shown in Fig. S9,† the variation of E' and the tan δ peak during the glass transition logically depends on the frequency of solicitation since a shift to higher temperature is observed between 0.1 and 10 Hz. We also observe a high Shore D value (used for hard rubbers) of 73 ± 3 at room temperature, since the material is partially in the glassy state, thus outperforming the hardness of ELO thermosets cured with MTHPA and other hard curing hardeners.[54]

The tensile properties of the cured resin were also investigated at room temperature, thus within the glassy region of the material. This resulted in a high tensile strength of 29 ± 2 MPa and observed Young's modulus of 467 ± 28 MPa (Table 1). Compared to linear bio-based diacids previously used to cross-link ELO such as suberic and adipic acid (Table 1), a far stronger material with similar strain at break was obtained. Using succinic acid, a particularly short diacid, a strong material with a relative high elongation at break (ε_B) can be obtained, which is however still softer and displays a lower tensile strength than **CBDA-2** cross-linked ELO. Using a bio-based anhydride such as glutaric anhydride can yield a highly cross-linked thermoset, with a high Young's modulus and tensile strength, yet extremely low ε_B of 3% compared to 30% with **CBDA-2**. This **CBDA-2** hardener thus competes very well with other petrobased hardeners (Table 1). The tensile strength with **CBDA-2** is almost comparable with those obtained when ELO is cured with 4,4′-methylenedianiline (classified in ECHA as a substance of very high concern requiring authorisation before it is used – carcinogenic and suspected to be muta-

genic) or with 4-methylhexahydrophtalic anhydride (corrosive and health hazard substance) despite a slightly lower modulus. ELO cured with CBDA largely surpass the ELO resin cured with 2,2′-dithiodibenzoic acid in term of tensile strength and elongation at break suggesting more ductile resins at ambient temperature. Consequently, **CBDA-2** positions itself as a suitable cross-linker for strong and durable vegetal oil-based thermosets avoiding health concerns associated with anhydride or amine curing agents.[55,56]

Conclusions

To meet the current demand to replace conventional fossil-based materials with sustainable alternatives, researchers are encouraged to find new chemicals that perform equally well, or better than conventional chemicals. The current work focused on employing a furfural-based sustainable hardener to cure epoxidized linseed oil (ELO), a widely used and promising epoxy matrix to obtain sustainable materials. Using typical hot curing processes, a furfural-based semi-rigid diacid, namely *cis*-cyclobutane-1,2-dicarbocylic acid, **CBDA-2**, was successfully used to cross-link ELO, yielding thermosets with excellent properties.

Curing characteristics resembled those of other materials cured with diacid or anhydride hardener, with a significant drop in the activation energy during the progressing reaction due to the diffusion processes becoming the rate limiting factor. The cured materials appeared very solid at room temperature, thanks to a high glass transition of the cured material, which also caused a high Shore D hardness level, characterizing the present material as a hard rubber material. A comparison with other known oil-based thermosets revealed that **CBDA-2** can lead to a material with superior strength, while retaining a good degree of toughness and strength at break. By using a simple method, a strong bio-based thermoset was obtained in a convenient manner, providing a potential alternative to fossil-based anhydride curing agents. This is also the first time that **CBDA-2** is employed as a 100% sustainable cross-linker to prepare bulky biobased thermoset materials – and not only coatings – which can then expand the

Table 1 Tensile testing data of cured thermoset prepared in this work in addition to previously published thermosets cured with natural diacids and anhydrides

	Linker	Tensile data			
		E (MPa)	σ_Y (MPa)	ε_B (%)	Toughness (J m^{-3})
Biobased	**CBDA-2**	467 ± 28	29 ± 2	30 ± 7	1.3 ± 0.4
	Succinic acid[34]	78 ± 9	11 ± 2	98 ± 9	—
	Suberic acid[34]	3.9 ± 0.2	0.6 ± 0.1	22 ± 2	—
	Adipic acid[19]	22 ± 0.1	8.8 ± 0.3	55 ± 1	
	Glutaric acid anhydride[22]	1477 ± 25	24 ± 1	3 ± 0.3	
Petrobased	2,2′-Dithiodibenzoic acid[43]	811 ± 36	10.9 ± 1	1.4 ± 0.1	
	4,4′-Methylenedianiline[57]	1500	41	30	
	4-Methylhexahydrophtalic anhydride[58]	2200	40	10	

With E = Young's modulus; σ_Y = tensile strength at yield point; ε_B = strain at break.

potential to processes such as compression molding, resin transfer molding, *etc.* with many applications in the emerging industry of green composites.

Abbreviations

DSC   Differential scanning calorimetry
DMTA   Dynamic mechanical thermal analysis
ELO   Epoxidized linseed oil
CBDA-2   *cis*-Cyclobutane-1,2-dicarbocylic acid.

Author contributions

The manuscript was written through contributions of all authors. All authors have given approval to the final version of the manuscript.

Conflicts of interest

The authors declare no conflict of interest.

References

1 R. Geyer, J. R. Jambeck and K. L. Law, *Sci. Adv.*, 2017, **3**, 1–5.
2 A. Fothergill, J. Hughes and K. Scholey, *David Attenborough: A Life On Our Planet*, 2020.
3 T. Werpy and G. Petersen, *Top value added chemicals from biomass Volume I—Results of screening for potential candidates from sugars and synthesis gas energy efficiency and renewable energy*, 2004.
4 Y. Wang, C. A. Brown and R. Chen, *AIMS Microbiol.*, 2018, **4**, 261–273.
5 M. Bicker, J. Hirth and H. Vogel, *Green Chem.*, 2003, **5**, 280–284.
6 C. M. Cai, T. Zhang, R. Kumar and C. E. Wyman, *J. Chem. Technol. Biotechnol.*, 2014, **89**, 2–10.
7 J. W. Döbereiner, *Ann. Pharm.*, 1832, **3**, 141–146.
8 R. Mariscal, P. Maireles-Torres, M. Ojeda, I. Sádaba and M. López Granados, *Energy Environ. Sci.*, 2016, **9**, 1144–1189.
9 G. Machado, S. Leon, F. Santos, R. Lourega, J. Dullius, M. E. Mollmann and P. Eichler, *Nat. Resour.*, 2016, **07**, 115–129.
10 H. E. Hoydonckx, W. M. Van Rhijn, W. Van Rhijn, D. E. De Vos and P. A. Jacobs, in *Ullmann's Encyclopedia of Industrial Chemistry*, Wiley-VCH Verlag GmbH & Co. KGaA, Weinheim, Germany, 2007.
11 S. Thiyagarajan, A. Pukin, J. Van Haveren, M. Lutz and D. S. Van Es, *RSC Adv.*, 2013, **3**, 15678–15686.
12 I. Delidovich, P. J. C. Hausoul, L. Deng, R. Pfützenreuter, M. Rose and R. Palkovits, *Chem. Rev.*, 2016, **116**, 1540–1599.
13 S. Rajagopalan, *Proc. – Indian Acad. Sci., Sect. A*, 1942, **16**, 163–166.
14 Z. Wang, B. Kastern, K. Randazzo, A. Ugrinov, J. Butz, D. W. Seals, M. P. Sibi and Q. R. Chu, *Green Chem.*, 2015, **17**, 4720–4724.
15 Z. D. Wang, Q. Elliott, Z. Wang, R. A. Setien, J. Puttkammer, A. Ugrinov, J. Lee, D. C. Webster and Q. R. Chu, *ACS Sustainable Chem. Eng.*, 2018, **6**, 8136–8141.
16 P. Muturi, D. Wang and S. Dirlikov, *Prog. Org. Coat.*, 1994, **25**, 85–94.
17 J.-M. Pin, N. Sbirrazzuoli and A. Mija, *ChemSusChem*, 2015, **8**, 1232–1243.
18 W. Knörr, P. Daute, R. Grützmacher and R. Höfer, *Fett Wiss. Technol.*, 1995, **97**, 165–169.
19 C. Ding, P. S. Shuttleworth, S. Makin, J. H. Clark and A. S. Matharu, *Green Chem.*, 2015, **17**, 4000–4008.
20 J. Tellers, P. Willems, B. Tjeerdsma, N. Guigo and N. Sbirrazzuoli, *Green Chem.*, 2020, **22**, 3104–3110.
21 P. Gogoi, M. Boruah, S. Sharma and S. K. Dolui, *ACS Sustainable Chem. Eng.*, 2015, **3**, 261–268.
22 C. Ding, G. Tian and A. Matharu, *Mater. Today Commun.*, 2016, **7**, 51–58.
23 H. J. Qi, K. Joyce and M. C. Boyce, *Rubber Chem. Technol.*, 2003, **76**, 419–435.
24 S. Vyazovkin, A. K. Burnham, J. M. Criado, L. A. Pérez-Maqueda, C. Popescu and N. Sbirrazzuoli, *Thermochim. Acta*, 2011, **520**, 1–19.
25 S. Vyazovkin, A. K. Burnham, L. Favergeon, N. Koga, E. Moukhina, L. A. Pérez-Maqueda and N. Sbirrazzuoli, *Thermochim. Acta*, 2020, **689**, 178597.
26 S. Vyazovkin and N. Sbirrazzuoli, *Macromol. Rapid Commun.*, 2006, **27**, 1515–1532.
27 S. Vyazovkin, in *Isoconversional Kinetics of Thermally Stimulated Processes*, Springer International Publishing, 2015, pp. 27–62.
28 N. Sbirrazzuoli, *Polymers*, 2020, **12**, 1280.
29 S. Vyazovkin, *J. Comput. Chem.*, 1997, **18**, 393–402.

30 N. Sbirrazzuoli, L. Vincent and S. Vyazovkin, *Chemom. Intell. Lab. Syst.*, 2000, **54**, 53–60.

31 S. Vyazovkin, *J. Comput. Chem.*, 2001, **22**, 178–183.

32 N. Sbirrazzuoli, *Thermochim. Acta*, 2013, **564**, 59–69.

33 N. Sbirrazzuoli, L. Vincent and S. Vyazovkin, *Chemom. Intell. Lab. Syst.*, 2000, **52**, 23–32.

34 C. Menager, N. Guigo, L. Vincent and N. Sbirrazzuoli, *J. Polym. Sci.*, 2020, **58**, 1717–1727.

35 A. Cadenato, J. M. Salla, X. Ramis, J. M. Morancho, L. M. Marroyo and J. L. Martin, *J. Therm. Anal.*, 1997, **49**, 269–279.

36 H. Teil, S. A. Page, V. Michaud and J. A. E. Månson, *J. Appl. Polym. Sci.*, 2004, **93**, 1774–1787.

37 S. Vyazovkin and N. Sbirrazzuoli, *Macromolecules*, 1996, **29**, 1867–1873.

38 N. Sbirrazzuoli, A. Mititelu-Mija, L. Vincent and C. Alzina, *Thermochim. Acta*, 2006, **447**, 167–177.

39 H. Amjaour, Z. Wang, M. Mabin, J. Puttkammer, S. Busch and Q. R. Chu, *Chem. Commun.*, 2019, **55**, 214–217.

40 P. D. Flory, *Principles of Polymer Chemistry*, Cornell University Press, Ithaca, 1953.

41 N. Sbirrazzuoli, *Molecules*, 2019, **24**, 1683–1699.

42 N. Sbirrazzuoli, S. Vyazovkin, A. Mititelu, C. Sladic and L. Vincent, *Macromol. Chem. Phys.*, 2003, **204**, 1815–1821.

43 C. Di Mauro, S. Malburet, A. Genua, A. Graillot and A. Mija, *Biomacromolecules*, 2020, **21**, 3923–3935.

44 J. M. España, L. Sánchez-Nacher, T. Boronat, V. Fombuena and R. Balart, *J. Am. Oil Chem. Soc.*, 2012, **89**, 2067–2075.

45 A. R. Mahendran, G. Wuzella, A. Kandelbauer and N. Aus, *J. Therm. Anal. Calorim.*, 2012, **107**, 989–998.

46 I. M. Barszczewska-Rybarek, A. Korytkowska-Wałach, M. Kurcok, G. Chladek and J. Kasperski, *Acta Bioeng. Biomech.*, 2017, **19**, 47–53.

47 T. Murayama and J. P. Bell, *J. Polym. Sci., Part A-2*, 1970, **8**, 437–445.

48 N. Doroudgarian, L. Pupure and R. Joffe, *Polym. Compos.*, 2015, **36**, 1510–1519.

49 L. Pupure, N. Doroudgarian and R. Joffe, *Polym. Compos.*, 2014, **35**, 1150–1159.

50 N. Ghasemi Rad, Z. Karami, M. J. Zohuriaan-Mehr, A. Salimi and K. Kabiri, *Polym. Adv. Technol.*, 2019, **30**, 2361–2369.

51 H. Miyagawa, A. K. Mohanty, M. Misra and L. T. Drzal, *Macromol. Mater. Eng.*, 2004, **289**, 629–635.

52 N. Boquillon and C. Fringant, *Polymer*, 2000, **41**, 8603–8613.

53 S. K. Sahoo, V. Khandelwal and G. Manik, *Polym. Adv. Technol.*, 2018, **29**, 2080–2090.

54 K. Thiele, N. Eversmann, A. Krombholz and D. Pufky-Heinrich, *Polymers*, 2019, **11**, 1409.

55 R. Schöneich and G. Wallenstein, *Z. Gesamte Hyg.*, 1990, **36**, 164–166.

56 Y. I. Li, F. Xiao, K. S. Moon and C. P. Wong, *J. Polym. Sci., Part A: Polym. Chem.*, 2006, **44**, 1020–1027.

57 J. D. Earls, J. E. White, L. C. López, Z. Lysenko, M. L. Dettloff and M. J. Null, *Polymer*, 2007, **48**, 712–719.

58 T. Tsujimoto, K. Takeshita and H. Uyama, *J. Am. Oil Chem. Soc.*, 2016, **93**, 1663–1669.